Overview of the Elastic Scattering Analysis at Braidwood

May 20, 2005

This document provides an overview of the status of the Elastic Scattering analysis which is proposed for the Braidwood experiment. Our goal is to make a measurement of the neutrino neutral current weak couplings at a level competitive with the $\sin^2\theta_W$ measurement from the NuTeV deep inelastic scattering experiment, but with substantially different systematics. This is equivalent to an elastic scattering measurement which is four times better than the best previous result. This is clearly an ambitious goal.

What we propose is a state-of-the-art measurement. Below, we show that this goal is well motivated by the physics. We then discuss the progress we have made in identifying methods to reduce error to meet the goal. In many cases, we describe work in progress. Therefore, this discussion should not be taken as a final estimate of the errors. While we believe that the estimates are reasonably well-founded, there is still a great deal of simulation-work, bench-testing and in-situ studies to be done.

The results presented here update Reference [1], which was written before Braidwood had developed its baseline design. Here, the estimate for sensitivity is derived from the baseline design described in the NSF proposal and presented to NuSAG. Also, here we present many new ideas for approaching some of the most difficult errors and issues.

1 Physics Motivation

The physics motivation for the Braidwood elastic scattering analysis arises from the NuTeV anomaly, a 3σ deviation of $\sin^2\theta_W$ from the Standard Model prediction [2]. This was measured in deep inelastic neutrino scattering ($Q^2 = 1$ to 140 GeV^2, $\langle Q^2_\nu\rangle = 26$ GeV^2, $\langle Q^2_{\bar\nu}\rangle = 15$ GeV^2). A similar deviation has been seen in past neutrino experiments (see Figure 1), however NuTeV is the first result of sufficient precision to indicate a clear anomaly.

Since the NuTeV result was published in 2001, over 225 papers have been written addressing the result, and a compendium can be found at reference [3]. There have been no criticisms of the experimental technique; instead the controversy has focussed on the theoretical inputs to the analysis. These "Standard Model Explanations" for the NuTeV anomaly

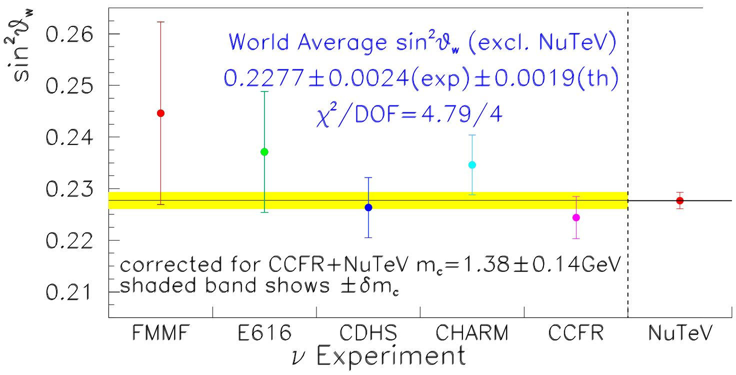

Figure 1: Measurements of $\sin^2\theta_W$ from past experiments compared to NuTeV. The standard model value is 0.2227

.

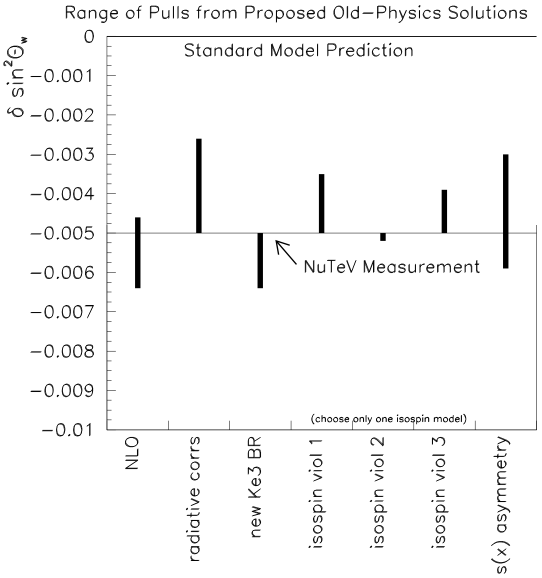

Figure 2: Pulls for "Standard Model Explanations" for the NuTeV anomaly. The three isospin violating models are mutually exclusive. The radiative correction model has yet to be successfully implemented by any group but the authors and is controversial.

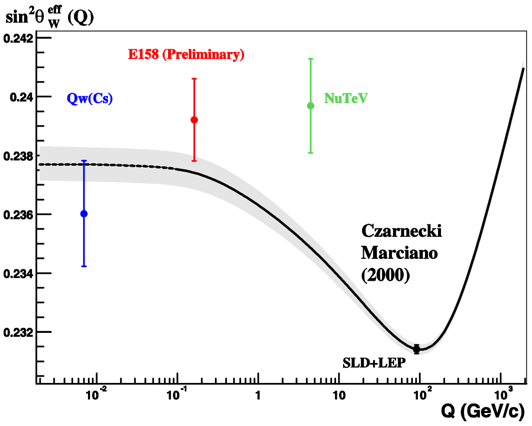

Figure 3: Measurements of $\sin^2\theta_W$ from reference [5]

.

have included recalculated radiative corrections (which are not fully tested), improved K_{e3} branching ratio, various models for isospin violation, and an asymmetric strange sea. As can be seen in Figure 2, however, these explanations result in pulls both toward and away from the Standard Model. And while some theorists have selectively chosen to consider only the pulls which go in the "right" (*i.e.* Standard Model) direction, this is not a sensible approach.

Other results of lesser significance, when considered within the context of the NuTeV anomaly, increase the interest in the question. Taken at face value, the NuTeV anomaly indicates a reduction in the coupling of the Z to neutrinos compared to other leptons. This is consistent with the LEP I measurements[4] of $Z \to \nu\bar{\nu}$ at the Z pole, which measure the number of neutrinos to be $3 \times (0.9947 \pm 0.0028)$. This is 2σ lower than the Standard Model prediction and consistent with NuTeV. Recently, the SLAC E158 experiment has also seen a deviation in $\sin^2\theta_W$ (see Fig 3) which is substantially less significant than NuTeV, but in the same direction [5].

An experiment which could address this question can have very large physics return. In light of the above, one can define the features of the best follow-up experiment. Various Beyond-the-Standard Model explanations have been put forward [3], and those which best explain the result require [6, 7] a follow-up experiment which probes the neutral weak couplings specifically with neutrinos. Because the Standard Model Explanations for the NuTeV result have largely focussed on the quark vertex, the ideal follow-up would avoid questions of QCD corrections. Also, because the NuTeV beam flavor-content has figured in both Standard Model Explanations (the K_{e3} branching ratio) and Beyond-the-Standard Model Explanations (see reference [8]), it would be best to use an entirely different neutrino source.

The Braidwood near detectors offer an opportunity to address the question of NuTeV anomaly. This analysis has been developed within the baseline of the Braidwood experiment

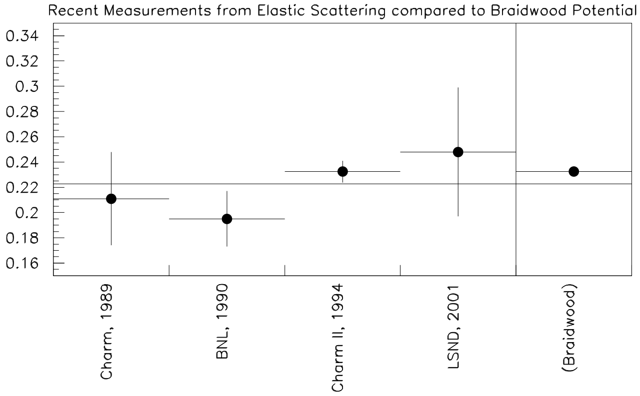

Figure 4: Measurements of $\sin^2\theta_W$ from $\nu_\mu e$ scattering experiments compared to the expectation for Braidwood ($\bar{\nu}_e e$ scattering), aligned with the NuTeV result.

and thus represents substantial additional physics capability without additional cost.

2 Technique for Measuring the WMA

In Reference [1], we outlined a plan for measuring $\sin^2\theta_W$ at ($Q^2 \approx 0$) at Braidwood. Here we have developed these ideas further and adapted them to the present Braidwood baseline.

In a reactor-based experiment, the weak mixing angle can be extracted from the purely leptonic $\bar{\nu}e$ "elastic scatter" (ES) rate, which is normalized using the $\bar{\nu}p$ "inverse beta decay" (IBD) events, to reduce the error on the flux. Thus a hydrocarbon (scintillator oil) based detector, which has free proton targets for the IBD events, is ideal. Gadolinium (Gd) doping is necessary for a high rate of neutron capture, the signal for the IBD events. A window in visible energy of 3 to 5 MeV is selected to reduce backgrounds from contaminants in the oil and cosmic-muon-induced isotopes. In this range the contamination which contributes is U and Th.

Our paper [1] showed that a combination of large overburden and high reactor neutrino rate is crucial to the measurement. Of the oscillation experiments proposing to run in the near future, only Braidwood can make a competitive measurement. This is because only Braidwood has near detectors with both sufficient overburden and sufficient proximity to the source. The expected error on $\sin^2\theta_W$ from Braidwood ~ 0.0019.

Neutrino magnetic moment experiments also exploit elastic scattering. The difficulties of these searches have led to skepticism concerning this analysis. However, several aspects of this analysis are substantially simpler than the traditional analyses for neutrino magnetic moment experiments. First, this measurement can be done at high visible energy (> 3 MeV), therefore the backgrounds are less. The high energy window allows this to be a relative measurement, not an absolute measurement, since the neutrinos have energies above IBD threshold. By doing a relative measurement, many errors cancel. Lastly, there is no need for tracking, only energy measurement.

The goal of the analysis is four times smaller errors than the past best elastic scattering measurement. This measurement, from CHARM II, was from $\nu_\mu e$ elastic scattering and is 0.2334 ± 0.0086 [11], which, like NuTeV, is high with respect to the Standard Model. A comparison of recent elastic scattering measurements is shown in Figure 4. The horizontal line indicates the Standard Model expectation. The expectation for Braidwood is also shown, aligned with the NuTeV value. It should be noted that this is $\bar{\nu}_e e$ scattering, so is a somewhat different measurement than the others, from a theoretical point of view. Braidwood represents an order of magnitude improvement over past $\bar{\nu}_e e$ scattering experiments.

3 Errors Used in Calculating the Sensitivity

One should see Reference [1] for details of the issues in the analysis. The main errors in the analysis arise from 1) statistics on the signal, 2) statistics and systematics on the misidentified IBD events, 3) statistics and systematics on the subtraction of the background from contamination, 4) systematics on the fraction of IBD events captured by the Gd, 5) statistics and systematics on the muon-induced isotopes, 6) systematics on the number of targets (the electron-to-free proton ratio), 7) systematics on the relative fiducial volume for ES versus IBD events, and 8) systematics on the energy scale. The simplest way to present the error is as the fractional error on the measured number of ES events, dN/N. We consider each in turn below, first stating the goal and then explaining why we believe we can achieve this goal.

3.1 Statistical Error on ES Events

Goal: $(dN/N)_{stat} = 0.6\%$

At a horizontal distance of 200 m and 450 mwe depth, in a run of 900 days, 24k ES events are expected in the energy window. This leads to the statistical uncertainty quoted above.

3.2 IBD Misidentification

Goal: $(dN/N)_{IBD} = 0.7\%$

Three million IBD events will be in the energy window and four million are produced above 3 MeV in a 900 day run. IBD events are identified by the capture of the neutron on H or Gd in the oil. Because the main analysis cuts 30 cm from the edge of the acrylic vessel, the neutron is lost in very few IBD events. The neutron pathlength is approximately 6 cm, however the neutron is not identified until the resulting photons deposit energy through Compton scatters. In CHOOZ, the pathlength between positron and neutron-identified-position was 20 cm. Neutrons may also be lost because of captures outside of the search window in time. The inefficiency leading to mid-identification is expected to be 1%. The statistical error on the misidentifications is the square root of the number divided by the number of ES events.

It is important to identify methods to accurately measure IBD misidentification, in order to reduce the systematic error on this term to a negligible level. A speculative idea which is under study is to use the positron hit timing in order to identify a pure sample of about 10% of IBD events. This is an extension of the method described in the next section.

3.3 Contamination of the Gd

Goal: $(dN/N)_{Gd`con} = 0.3\%$

The issue of producing highly purified Gd for doping in the detector was not addressed in Reference [1]. Based on work presented at the LRT2004 conference[13], given an ∼0.1% concentration, $\sim 10^{-15}$ g/g of Th background should be achievable. This is sufficient for the analysis, but it would be better for this to be reduced.

A possible method of further reducing the background is to exploit the fact that the main daughter product which causes background, ^{208}Tl, has a topology that is significantly different from an ES event. This is a speculative idea, but one which appears to be promising.

A relatively high energy photon, of 2.6 MeV, is always produced in this decay. In the case where the photon exits, the background moves out of the energy window of the analysis. Recent studies for Braidwood have shown that a large fraction of the remaining events may be identified through hit timing. This method finds the vertex using only the charge, and then asks if the hit-timing is consistent with the vertex position. The presence of high energy photons, which must Compton scatter to deposit energy, often results in late hits at the phototubes.

With a realistic scintillator (either PPO, which is used in Borexino, or Butyl PBD, which was used in LSND) a rejection factor ~ 100 of ^{208}Tl events can be obtained while maintaining 90% of the ES events. Figure 5 shows the separation obtained using a likelihood analysis. This analysis assumed that only the time of the first hit at the tube is recorded. If the electronics for Braidwood is fast-digitizing as discussed in the previous section, this separation may improve. The stated error goal above is based on the assumption that we achieve a factor of 100 rejection.

As discussed in the previous section, it is possible that a similar analysis of IBD events can give some, albeit much poorer, separation from ES events. Since the goal is a pure sample of about 10% of the mis-IDs, this poor separation may be sufficient. Also some improvement may be gained from assuming fast digitization. This is under investigation.

3.4 The Gd Capture Fraction

Goal: $(dN/N)_{capture} = 0.3\%$

This is measured from the ratio of peaks for neutron capture, comparing the 2.2 MeV peak from H capture to the peak ~ 8 MeV for Gd capture. The error on the capture fraction comes from ability to separate the peaks. It is limited by statistics for measuring the capture

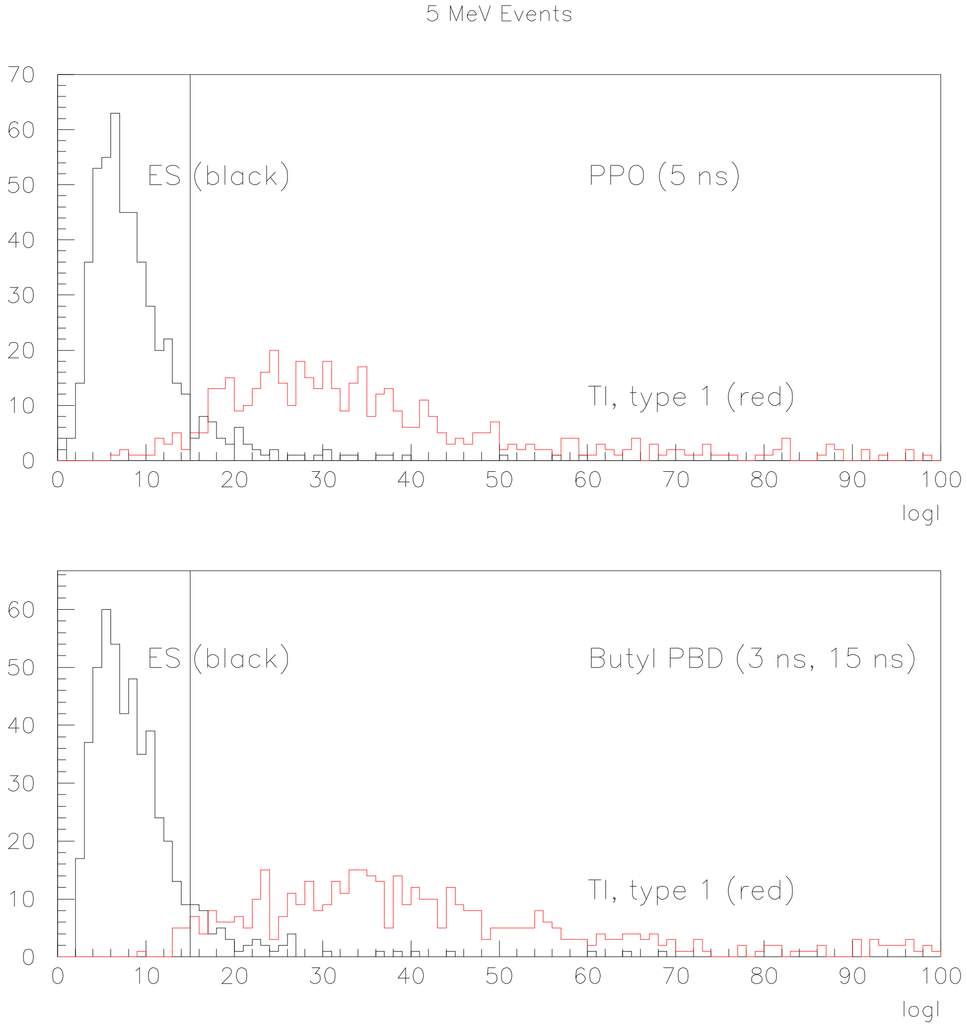

Figure 5: Comparison of the log likelihood of the reconstructed timing distribution for ES events (black) and the most likely decay mode of ^{208}Tl (red). The proposed cut is indicated by the line. Top: PPO. Bottom: Butyl PBD. We find similar rejection for the other ^{208}Tl decay modes.

ratio using a source. We assume a factor of two improvement in knowledge of the Gd capture fraction beyond CHOOZ based on longer running time with the source.

Note that in this analysis, because we cut 30 cm from the edge of the acrylic to define the fiducial volume, we do not expect a substantial loss of energy from the n-capture due to exiting particles. Thus we expect the peaks to be well-resolved. This question will be investigated further in the future.

If the hit-timing tag for IBD events is successful, this allows for alternative methods of identifying events with neutron captures that will have very small error. Therefore we believe that the stated goal, in this case, is likely to be exceeded.

3.5 Muon-induced Isotopes

Goal: $(dN/N)_{isotopes} = 0.2\%$

Because of the depth and the use of a muon-hadron veto, the error from the muon-induced isotopes at Braidwood will be small. The highest rate production is of ^{12}B, which is due to neutron interactions, $n+^{12}\text{C}\rightarrow p+^{12}\text{B}$. This beta decays with a lifetime of 20 msec with an endpoint of ~ 13 MeV. The rate will be 30k events over a period of 900 days in the energy window.

To cut these, we introduce a muon-hadron veto. As has been demonstrated in KamLAND, muons which produce ^{12}B are associated with high energy deposit in the detector [14]. The energy level will be set such that all but 10% of the ^{12}B events will be cut. Based on KamLAND, this threshold is expected to be at the energy associated with one full pathlength of muon in the active inner region of the detector. The veto window will be greater than 0.1 s, or 5 ^{12}B lifetimes, assuring that a very high fraction of the decays are identified by the veto. The deadtime for this veto should be tolerable. KamLAND has seen that only 2% of the throughgoing muons produce neutrons [15], thus of the 5 Hz of through going muons, only 0.1 Hz will fire the veto, leading to a 1% deadtime. The result is that 3000 ± 54 events are expected to pass the muon-hadron veto, which is a tolerable rate. Note that the stated error goal listed above requires that the muon-hadron veto be successful.

There are other contributions from long-lived spallation produced isotopes, which are at a lower level than the ^{12}B. These are ^{9}Li, ^{8}He, ^{8}Li , ^{9}C , ^{8}B, all of which have endpoints above 10 MeV; and ^{6}He, which has an endpoint at 3.5 MeV. The systematic error assigned to these is from Reference [16]. Only decays within the energy window and outside of the veto timing window are considered. Those with accompanying neutrons or identifiable α's in the decay are eliminated. For a full description of how these are handled see Reference [1].

3.6 Electron-to-Free Proton Ratio

Goal: $(dN/N)_{e/p} = 0.1\%$

Based on the CHOOZ knowledge of the number of free protons, the error on the electron-to-free proton ratio is 0.6%. (Note that the number of free protons and the electron-to-free proton-ratio are correlated). The CHOOZ error was determined through burning the oil. However, CHOOZ did not work hard to reduce this error because it was unnecessary for this analysis [17]. We will achieve a substantially better error using a combination of ex-situ and in-situ methods. The three types of ex-situ measurements use NMR, gas chromatography and heat-of-combustion techniques. These are each expected to achieve a measure the free protons to 0.3% by weight. The in-situ method using the n capture time, first developed by CHOOZ [18], and extended for the Braidwood θ_{13} measurement should achieve a similar level. Combining these measurements will lead to a negligible error from this source. In summary, we believe that the stated goal for this error is straightforward to reach.

3.7 Fiducial Volume Error

Goal: $(dN/N)_{relative\ fiducial} = 0.4\%$

The standard analysis plan calls for a fiducial volume cut away from the acrylic containment vessel. This reduces background from contamination and increases efficiency for capture of the neutrons in IBD events.

The fiducial volume error is then the error on the relative vertex reconstruction of ES vs. IBD events. This error could come about because the annihilation photons in the IBD events might lead to a pull in the vertex reconstruction. The error on the ES rate is given by $3dr/r$; thus a 3 mm relative error would lead to a 0.4% error in a detector with a 240 cm inner radius.

The concern with this method is that, so far, no in-situ tests have been identified which demonstrate this relative error in the detector. Thus, at present this error estimate relies upon Monte Carlo. Here we present ideas which are being pursued.

An alternative analysis eliminates the fiducial volume error entirely by using the acrylic sphere to define the fiducial region, however the rate of mis-identified IBD events rises substantially. Thus it represents a trade in the type of systematic error which dominates the analysis. We are presently studying the level of systematic error we can assume on the mis-identified IBD events, however this appears likely to be the dominant error associated with this technique. Our goal is to reach an error level which, although less precise than the first technique, provides a useful verification of the stability of the $\sin^2\theta_W$.

The analysis with no fiducial volume error employs the following procedure. First, one finds the shape of the IBD event distribution versus energy by cutting far from the acrylic sphere. Second, that distribution is normalized to the total IBD events in the acrylic, identified by the presence of a neutron. To obtain the total, all IBD events with visible energy above 0.5 MeV are simply counted. Since an IBD event must, at minimum, produce 1 MeV of energy in the form of annihilation photons, in principle, this counts 100% of the IBD events. In practice, there will be an inefficiency from annihilation photons leaving the scintillator-doped region defined by the acrylic vessel. However, this inefficiency is almost

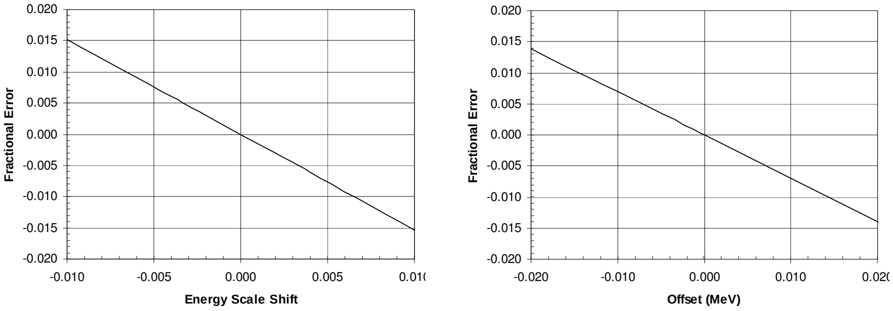

Figure 6: Effect of a relative error in energy calibration between IBD and ES events. Left: a difference in the energy scales; Right: a difference in the energy offsets.

independent of reasonable variations in the understanding of the edge of the acrylic vessel. So the systematic error from this is negligible. Lastly, one divides by the IBD cross section to isolate $flux \times targets$, which is then used to extract the predicted ES cross section.

A second method would introduce acrylic balls into the tank with $< 3mm$ cavities containing the Gd-doped liquid scintillator and dissolved β^+ and β^- sources. The vertex position of the sources would be reconstructed. A pull in the IBD events relative to the ES events would result in a broadening of the vertex distribution. At this point, the best choice of sources has not been identified.

In summary, we can show through Monte Carlo that the relative error should be small. However, we are still in the process of understanding how to constrain that error through in-situ tests.

3.8 Energy Offset/Scale Error

Goal: $(dN/N)_{offset/scale} = 0.7\%$

The relative error in the energy scale of ES vs. IBD events is by far the most difficult error to address in the analysis. Unlike most other errors, there is not a strong cancellation from using IBD events to normalize the ES events, because the event rates are changing in significantly different ways with energy. This is illustrated in Figure 6, which shows the error on the ES rate as a function of energy scale (left) and offset (right).

Our plan is to calibrate in a series of steps. The first step sets the IBD absolute energy scale and offset. This is tuned on the rising edge of IBD spectrum, which is very sensitive. With five million IBD events, we expect to achieve $\sim 0.1\%$ absolute scale error and $\sim$3 keV offset. The next step is to tune the relative offset between e^- and e^+ events. This is done using the michel electrons and positrons from muon decay. The presence of the annihilation photons leads to a 1 MeV offset in visible energy for the positron decay. Thus there is a kink in the overall spectrum which is sensitive to the offset. The scale error cannot be differentiated from the relative normalization error in this sample, and the relative normalization error is left as a free parameter. This results in a relative offset between e^- and e^+ events of about 5 keV. The final step is to fit for the scale error. We believe that the best way to approach this is by fitting β^- decays in the energy range of interest. Using only ^{6}He and ^{1}2B events, we can achieve 1% on the relative energy scale. This is low in statistics by about a factor of four from our stated goal above. More R&D is needed to identify β decaying elements which can be used to constrain the energy scale.

3.9 Total Error

At present, assuming 900 days of running, the estimated total error is $(dN/N)_{tot} = 1.3\%$, and on $\sin^2\theta_W$ is 0.0019. The error quoted here may change as we learn more about constraining the errors. This is to be expected from an analysis in development. However, we believe that this is a reasonably good estimate. This is comparable to the NuTeV error of 0.0016, and thus the measurement should be quite interesting.

References

[1] J. M. Conrad, J. M. Link and M. H. Shaevitz, Phys. Rev. D **71**, 073013 (2005) arXiv:hep-ex/0403048.

[2] G. P. Zeller *et al.* Phys. Rev. Lett., **88** 091802, 2002.

[3] http://home.fnal.gov/ gzeller/nutev.html

[4] http://lepewwg.web.cern.ch/LEPEWWG; The LEP Electroweak Working Group, hep-ex/0112021.

[5] R. Carr *et al.* SLAC-PROPOSAL-E-158. 1997.

[6] T. Takeuchi and W. Loinaz, arXiv:hep-ph/0410201.

[7] J. L. Rosner, Phys. Rev. D **70**, 037301 (2004) arXiv:hep-ph/0404264.

[8] J. S. Ma, J. M. Conrad, M. Sorel and G. P. Zeller, arXiv:hep-ex/0501011, submitted to Phys. Rev. Brief Reports.

[9] http://mwtheta13.uchicago.edu/index.html

[10] http://www.lngs.infn.it/site/exppro/panagic/sections/particle/experiments/knl.html

[11] P. Vilain, *et al.*, Phys. Lett. B335: 246, 1994.

[12] J.M. Moss, *et al.*, “Applications of Antineutrino Detector Technology to Counterterrorism,” Physics Div. Research Review, LA-14112-PR.

[13] http://lrt2004.snolab.ca/ see talk by M. Yeh

[14] G. Gratta, private communication (plot will soon appear in thesis by J. Detweiler).

[15] D-M Mei, ‘Measurement of Cosmic-Ray Muon-Induced Processes at the Kamland Neutrino Experiment,” Thesis, University of Alabama (2003).

[16] T. Hagner *et al.* Astropart. Phys., **14** 33–47, 2000.

[17] L. Mikaelyan, private communication.

[18] B. Lefievre, L. Mikaelyan, and V. Sinev, “Determination of Hydrogen Atom Concentration in the CHOOZ Gadolinium Loaded Scintillator,” College de France, LPC 94 49.